Journal of Applied Electrochemistry (2005) 35:1059–1065
DOI 10.1007/s10800-005-9015-9

The effect of electrolyte flow rate and temperature on corrosion and protection of Al–2.5 Mg alloy by (+)-catechin

LADISLAV VRSALOVIĆ, MAJA KLIŠKIĆ*, JAGODA RADOŠEVIĆ and SENKA GUDIĆ
Department of Electrochemistry and Materials Protection, Faculty of Chemical Technology, Teslina 10/V, 21000, Split, Croatia
*(*author for correspondence, fax: +385-21-384770, e-mail: kliskic@ktf-split.hr)*

Received 11 January 2005; accepted in revised form 18 May 2005

Key words: Al–2.5Mg alloy, corrosion, corrosion inhibition, flow conditions, (+)-catechin

Abstract

The effects of flow rate and temperature on the corrosion behaviour of the Al–2.5 Mg alloy in a 3% NaCl solution and the inhibiting efficiency of (+)-catechin on the corrosion of the same alloy have been examined. Measurements were carried out in a flow-through cell, at different flow rates ($v_1 = 0.0029$ m s^{-1}, $v_2 = 0.0059$ m s^{-1} and $v_3 = 0.0118$ m s^{-1}) and temperatures (20, 30, 40 °C). Electrochemical parameters for the Al–2.5 Mg alloy were determined by polarisation techniques and electrochemical impedance spectroscopy (EIS). Increased flow rate and temperature cause a stronger corrosion attack on the alloy. The addition of (+)-catechin inhibited corrosion at all temperatures and flow rates. The inhibitor efficiency decreased with increase in flow rate and temperature.

1. Introduction

Aluminium and its alloys have great economic and industrial importance owing to their low weight, high thermal and electrical conductivity and low cost. Aluminium-magnesium alloys are widely applied in shipbuilding, chemical and food-processing industry. Good corrosion resistance of Al and its alloys is attributed to the presence of the thin protective surface oxide film. This oxide film is relatively stable in the range from pH 4 to 9 but in the presence of aggressive anions even in this pH range, protective layer can be locally destroyed and corrosive attack may take place [1–3].

One of the methods for metal and alloy corrosion protection is the application of corrosion inhibitors [3–12]. The increasing awareness of health and ecological risks has turned attention to finding suitable inhibitors, which are non-toxic. Therefore, the inhibiting properties of amino acids and hydroxy carboxylic acids [13, 14], vanillin [15] and other organic compounds obtained from plants [16–18] are being examined.

In our previous study, we have examined the corrosion of the Al–2.5 Mg alloy in a stationary 3% NaCl solution and its inhibition by a polyphenolic compound (+)-catechin [16]. It is known that many, if not most, cases of corrosion involve some relative motion between the corroding metal and its environment. Such movements can increase or decrease the processes occurring under static conditions and can also introduce different types of attack [19, 20]. Above the critical flow rate, corrosion inhibitors may lose their effectiveness, which depends of the nature and molecular structure of the inhibitor as well as on its concentration and temperature. Therefore, the aim of this work has been to study the effect of the electrolyte flow rate and temperature on corrosion and corrosion inhibition on the Al–2.5 Mg alloy in a 3% NaCl solution by means of (+)-catechin.

2. Experimental

In all experiments, the Al–2.5 Mg alloy cylinder sample was made into an electrode by inserting insulated aluminium wire and protecting all sides but one with epoxy resin. The exposed geometric area was 0.5 cm^2. Table 1 shows the chemical composition of the alloy. Before to each experiment the electrode surface was mechanically polished with emery paper to an 1200 metalographic finish, degreased in ethanol, rinsed with doubly distilled water and left a few minutes in the air to develop the ''natural'' oxide film prior to its introduction into the measuring cell.

The basic solution was deaerated 3% NaCl, to which the additive was added in concentrations 1×10^{-4} and 1×10^{-5} mol dm^{-3}. The (+)-catechin isolated from the first neutral subfraction of the aqueous extract of

Table 1. Chemical composition of the Al–2.5Mg alloy (wt.%)

Element	Composition
Si	0.19
Fe	0.40
Cu	0.06
Mn	0.27
Mg	2.59
Cr	0.02
Zn	0.04
Ti	0.02
rest	0.1
Al	Balance

rosemary leaves was used as the inhibitor [16]. The usefulness of (+)-catechin is important for economic reasons and for health protection, because it has been acknowledged an antioxidant and radical scavenger [21, 22].

Electrochemical investigations were performed under the flow conditions with equipment specially designed for this kind of measurements [23]. The difference in our equipment lay in the entry and exit regions of the flow-through cell, which was conically shaped instead of rounded. A saturated calomel electrode (SCE) with a Luggin capillary was used as the reference and Pt plate as the counter electrode.

The experiments were performed at flow rates of $v_1 = 0.0029$ m s^{-1}, $v_2 = 0.0059$ m s^{-1} and $v_3 = 0.0118$ m s^{-1} and in the temperature range of 20–40 °C. The Reynolds number was calculated according to the relation:

$$\mathrm{Re} = \frac{v\mathrm{d}\rho}{\mu} \quad (1)$$

where v is the electrolyte velocity (m s^{-1}), d the cell diameter (m), ρ the electrolyte density (10^3 kg m^{-3}) and μ the electrolyte viscosity (10^3 Pa s). The lower limit for laminar to turbulent transition is Re ~2000 [19]. The calculated Reynolds number values ($\mathrm{Re}_1 = 200$, $\mathrm{Re}_2 = 400$ and $\mathrm{Re}_3 = 800$) confirm that the experiments were performed under laminar flow conditions. Potentiodynamic polarization measurements were performed using a potentiostat (PAR M 273A), with the scanning rate of 0.2 mV s^{-1}. Anodic and cathodic branches of polarization curves were recorded and in the form of a Tafel diagram. Corrosion parameters from the polarization curves were calculated using cathodic Tafel lines. The polarization resistance, R_p, was determined from the slope of polarization curves obtained by measurements in the potential range from −10 mV to +10 mV from the corrosion potential and with a scan rate of 0.2 mVs^{-1}. For impedance measurements, a lock-in amplifier (PAR M5210) was also used. Impedance measurements were carried out at the open circuit potential (E_{OCP}) 30 min after the electrode had been immersed in the test solution. The a.c. amplitude was ±10 mV and the frequency range studied was from 100 kHz to 30 mHz.

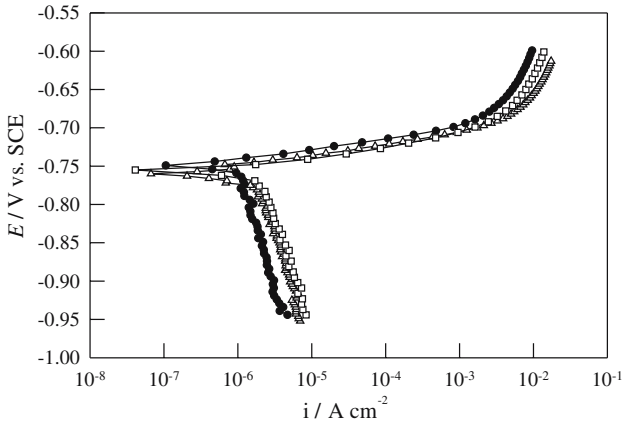

Fig. 1. Potentiodynamic polarization curves for the Al–2.5Mg alloy in a 3% NaCl solution at 20 °C and different flow rates: $v_1 = 0.0029$ m s^{-1} (●), $v_2 = 0.0059$ m s^{-1} (Δ) and $v_3 = 0.0118$ m s^{-1} (□).

3. Results and discussion

3.1. *Polarization measurements*

Figure 1 shows the potentiodynamic polarization curves for the Al–2.5 Mg alloy in a 3% NaCl solution at 20 °C and at different flow rates. It is evident that increase in electrolyte flow rate leads to some increase in cathodic current density, while the effect of the increased flow rate on the anodic dissolution of metal through the naturally formed oxide film is low. As the measurements were carried out in deaerated solution, the only cathodic reaction possible was hydrogen release, which develops very slowly by dissociation of water molecules catalysed by the Al_2O_3 film:

$$2H_2O \rightarrow H_3O^+ + OH^- \quad (2)$$

$$2H_3O^+ + 2e^- \rightarrow H_2 + 2H_2O \quad (3)$$

Table 2 shows the corrosion parameters for the Al–2.5 Mg alloy in a 3% NaCl solution at different temperatures and flow rates. Increase in flow rate and temperature has negligible effect on the corrosion

Table 2. Corrosion parameters for the Al–2.5Mg alloy in a 3% NaCl solution obtained by potentiodynamic polarization method

T/K	v/m s^{-1}	$-b_c$/V dec^{-1}	i_{corr}/μA cm^{-2}	E_{corr}/V
293	0.0029	0.3135	1.90	−0.748
	0.0059	0.2460	2.80	−0.759
	0.0118	0.2692	3.50	−0.755
303	0.0029	0.3212	2.70	−0.760
	0.0059	0.2731	3.40	−0.751
	0.0118	0.2654	5.10	−0.740
313	0.0029	0.2885	3.60	−0.761
	0.0059	0.3654	4.50	−0.744
	0.0118	0.3135	6.20	−0.751
318	0.0029	0.3227	4.12	−0.749

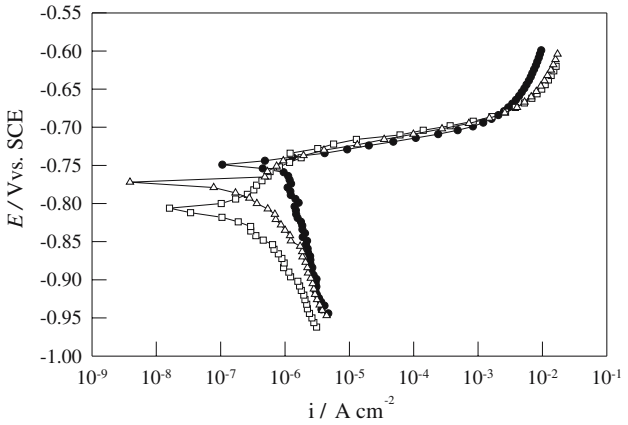

Fig. 2. Potentiodynamic polarization curves for the Al–2.5 Mg alloy in a 3% NaCl solution at 20 °C and the flow rate v = 0.0029 m s^{-1}, without (●) and with the addition of (+)-catechin in the concentration of 1×10^{-4} mol dm^{-3} (□) and 1×10^{-5} mol dm^{-3} (Δ).

potential, E_{corr}, but it is evident that at higher electrolyte flow rates and temperatures the corrosion current densities are higher. The effect of electrolyte flow rate on the inhibitory action of the additive was examined in a 3% NaCl solution to which (+)-catechin was added in concentrations of 1×10^{-4} mol dm^{-3} and 1×10^{-5} mol dm^{-3}. Figure 2 shows the potentiodynamic polarization curves for the Al–2.5 Mg alloy in a 3% NaCl solution in the absence and in the presence of the (+)-catechin at the temperature of 20 °C and flow rate of $v = 0.0029$ m s^{-1}. The results indicate that the addition of (+)-catechin causes major changes in the polarization behaviour. The added substance reduces the cathodic current density and shifts the corrosion potential in the negative direction. This difference decreases with increase in electrolyte flow rate and temperature, indicating lower inhibitory action of the (+)-catechin on the corrosion of the alloy examined under given conditions. The changes in polarization behaviour of the alloy due to addition of inhibitor, as in this case, are customary in inhibition of local corrosion attacks [24]. Table 3 shows the polarization parameters for the Al–2.5 Mg alloy in a 3% NaCl solution in the presence of (+)-catechin and also lists the percentages of inhibitor efficiency, which were calculated using the equation:

$$\eta = \frac{i_{corr} - (i_{corr})_{inh.}}{i_{corr}} \times 100 \qquad (4)$$

where i_{corr} and $(i_{corr})_{inh.}$ are the corrosion current densities in the absence and in presence of inhibitor. The table indicates that the efficiency of (+)-catechin as inhibitor of corrosion of the Al–2.5 Mg alloy in a 3% NaCl solution decreases with increase in flow rate at each temperature. Increase in temperature also reduces the inhibition efficiency.

The dependence of the corrosion current on temperature can be regarded as an Arrhenius type process [25], the rate of which is:

$$i_{corr} = A \exp\left(-\frac{E_a}{RT}\right) \qquad (5)$$

where i_{corr} is the corrosion current density, A is the Arrhenius preexponential constant, E_a is the apparent activation energy, R is the universal gas constant and T is the absolute temperature. In order to calculate E_a, additional polarisation measurements were performed at 45 °C. Figure 3 presents the Arrhenius plots of the logarithm of the corrosion current density vs. $1/T$ for a

Table 3. Corrosion parameters for the Al–2.5 Mg alloy in a 3% NaCl solution with addition of different concentration of (+)-catechin obtained by potentiodynamic polarization method

T/ K	v/m s^{-1}	$-b_c$/V dec^{-1}	i_{corr}/μA cm^{-2}	E_{corr}/V	η %
c((+)-catechin) = 1×10^{-4} mol dm^{-3}					
293	0.0029	0.1674	0.53	−0.804	72.10
	0.0059	0.2165	0.99	−0.804	64.46
	0.0118	0.2904	1.48	−0.764	57.71
303	0.0029	0.2076	1.08	−0.805	60.00
	0.0059	0.2154	1.50	−0.766	55.88
	0.0118	0.2981	2.41	−0.752	52.74
313	0.0029	0.2827	1.83	−0.748	49.16
	0.0059	0.3000	2.81	−0.749	37.55
	0.0118	0.3461	4.20	−0.750	32.26
318	0.0029	0.3381	2.37	−0.745	42.47
c((+)-catechin) = 1×10^{-5} mol dm^{-3}					
293	0.0029	0.2269	0.89	−0.771	53.16
	0.0059	0.2346	1.55	−0.772	44.64
	0.0118	0.2769	2.15	−0.754	38.57
303	0.0029	0.1815	1.35	−0.775	50.00
	0.0059	0.2750	1.99	−0.743	41.47
	0.0118	0.2750	3.30	−0.746	35.29
313	0.0029	0.2500	2.20	−0.757	38.89
	0.0059	0.2750	3.20	−0.755	28.89
	0.0118	0.3100	4.70	−0.741	24.19
318	0.0029	0.2873	2.76	−0.743	33.01

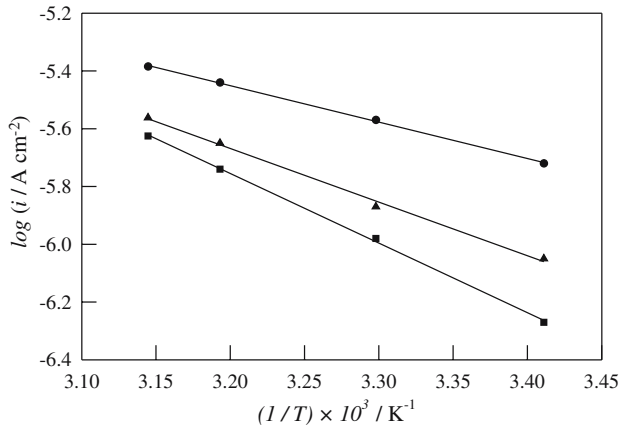

Fig. 3. Activation energy determination for the Al–2.5 Mg alloy in a 3% NaCl solution without (●) and with the addition of (+)-catechin in the concentration of 1×10^{-4} mol dm^{-3} (■) and 1×10^{-5} mol dm^{-3} (▲).

noninhibited 3% NaCl solution and with the addition of (+)-catechin. The E_a values were determined from the slopes of these plots and calculated to be:

$E_{a1} = 24.10$ kJ mol^{-1} in a noninhibited 3% NaCl solution.

$E_{a2} = 35.49$ kJ mol^{-1} with the addition of 1×10^{-5} mol dm^{-3} (+)-catechin.

$E_{a3} = 46.09$ kJ mol^{-1} with the addition of 1×10^{-4} mol dm^{-3} (+)-catechin.

Higher values of E_a in the presence of inhibitor indicate that a higher energy barrier is attained for the reaction [12].

Figure 4 shows the "linear" parts of polarization curves obtained by the linear polarization method for the Al–2.5 Mg alloy in a 3% NaCl solution without and with additive. Increase in inhibitor concentration leads to an increase in slope of the linear parts of the curves, i.e. to an increase in polarization resistance.

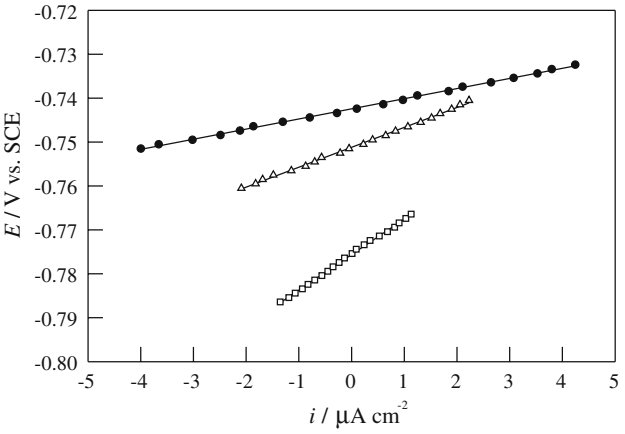

Fig. 4. "Linear" polarization curves for polarization resistance determination of the Al–2.5Mg alloy in a 3% NaCl solution at 20 °C and the flow rate $v = 0.0059$ m s^{-1} without (●) and with the addition of (+)-catechin in the concentration of 1×10^{-4} mol dm^{-3} (□) and 1×10^{-5} mol dm^{-3} (Δ).

The values of the polarization resistance, R_p, were determined from the slope of the "linear" polarization curves in the vicinity of E_{corr}:

$$R_p = \left(\frac{dE}{dI}\right)_{E=E_{corr}} \quad (6)$$

Since R_p is inversely proportional to the corrosion current, it can be used to calculate the inhibitor efficiency, η, using Equation (7):

$$\eta = 1 - \frac{R_{p,0}}{R_{p,i}} \quad (7)$$

where R_p,0 is the polarization resistance for the Al–2.5 Mg alloy in a 3% NaCl solution without inhibitor, and R_p,i is the polarization resistance in the presence of inhibitor. Table 4 lists the values of polarization resistance, R_p for the Al–2.5Mg alloy in uninhibited and inhibited solutions and the inhibiting efficiency, η.

Increase in electrolyte flow rate and temperature reduces the polarization resistance and the inhibiting efficiency.

3.2. *Electrochemical impedance measurements*

Figure 5 shows the Nyquist (a) and Bode (b) plots for the Al–2.5 Mg alloy in a 3% NaCl solution at the E_{OCP}. Two loops were observed in the Nyquist diagram: a capacitive loop at high frequencies and an inductive loop at low

Table 4. Polarization resistance and inhibition efficiencies for the Al–2.5 Mg alloy in a 3% NaCl solution without and with addition 1×10^{-4} mol dm^{-3} and 1×10^{-5} mol dm^{-3} of (+)-catechine at different temperatures and flow rates

c ((+)-catechine)/mol dm^{-3}	T/K	v/m s^{-1}	R_p/kΩ cm^2	η%
0	293	0.0029	3.08	
		0.0059	2.33	
		0.0118	1.57	
	303	0.0029	2.76	
		0.0059	2.00	
		0.0118	1.42	
	313	0.0029	2.05	
		0.0059	1.60	
		0.0118	1.11	
1×10^{-4}	293	0.0029	16.01	80.76
		0.0059	8.08	71.16
		0.0118	4.31	63.57
	303	0.0029	8.67	68.16
		0.0059	4.91	59.26
		0.0118	2.90	51.03
	313	0.0029	3.80	46.05
		0.0059	2.69	40.52
		0.0118	1.54	27.92
1×10^{-5}	293	0.0029	7.61	59.52
		0.0059	4.91	52.54
		0.0118	3.02	48.01
	303	0.0029	5.40	48.89
		0.0059	3.24	38.27
		0.0118	2.16	34.26
	313	0.0029	3.16	35.12
		0.0059	2.15	25.58
		0.0118	1.40	20.71

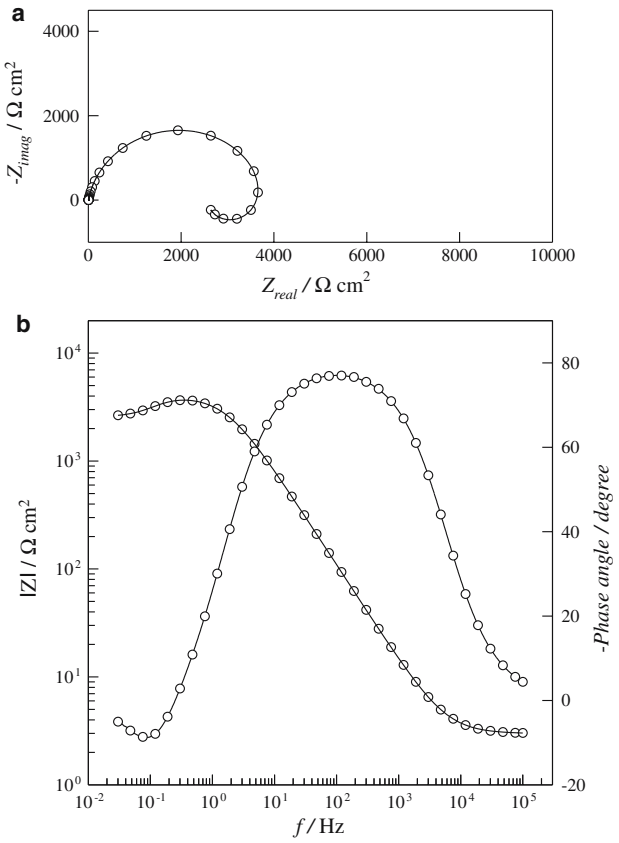

Fig. 5. Nyquist plot (a) and Bode plot (b) of the Al–2.5Mg alloy in a 3% NaCl solution at the E_{OCP} at 20 °C and the flow rate $v = 0.0029$ m s^{-1}.

frequencies. As far as the origin of different time constants is concerned, it can be concluded that there is no agreement. The capacitive time constant at high frequencies has often been attributed to the reactions involved in the formation of an oxide layer [26–28] or to the oxide layer itself [29–31]. An oxide film is usually considered to be a parallel circuit of resistance due to ionic conduction in the oxide and capacitance due to dielectric properties of the oxide. The origin of the inductive loop at low frequencies is also not clear. Burstein's measurements [32, 33] have confirmed that the inductive loop is closely related to the existence of a passive film on aluminium. Bessone et al. [29] have suggested that the inductive time constant is the result of rearrangement of the surface charge at the metal/oxide interface. Lendernik et al. [34] have attributed this loop to the relaxation of adsorbed intermediates in reduction of hydrogen like H^+_{ads}. An inductive loop is also observed for the pitted active state and attributed to the surface area modulation or salt film property modulation [28].

In the Bode plot, three distinctive segments can be observed. In the upper-frequency region, the log $|Z|$ vs. log f relationship approaches zero with the phase angle value of approximately 0°. This response is typical of the resistive behaviour and corresponds to the solution resistance. In the medium frequency region, a linear relationship is observed for log $|Z|$ vs. log f, with a slope close to −1 and phase angle values around −80°. In the low frequency region, inductive behaviour is observed with positive phase angle values (approximately 10°).

Figure 6 shows the effect of the (+)-catechin on the impedance spectra of the Al–2.5 Mg alloy in a 3% NaCl solution at E_{OCP}. The addition of (+)-catechin introduces changes in the impedance spectrum. In the Nyquist plot the diameter of the high frequency capacitive semicircle markedly increases with the addition of (+)-catechin, while the diameter and size of the inductive loop decrease, which probably reflects physical blocking of the alloy surface. In the Bode plot the addition of the inhibitor causes a significant increase in the value of the impedance modulus $|Z|$.

In the presence of inhibitor, the capacitive loop can be correlated with the dielectric properties of the surface (metal–oxide–inhibitor) adsorption layer, while the inductive loop can be attributed to the slow relaxation process of hydrogen and Cl^-, as well as to aluminium dissolution.

Figure 7 shows the effect of the flow velocity of the 3% NaCl solution in the presence of (+)-catechin of concentration of 1×10^{-5} mol dm^{-3} on the impedance diagrams. The spectra obtained indicate that impedance changes with the electrolyte flow rate. Changes are observed in the reduced diameter and size of the

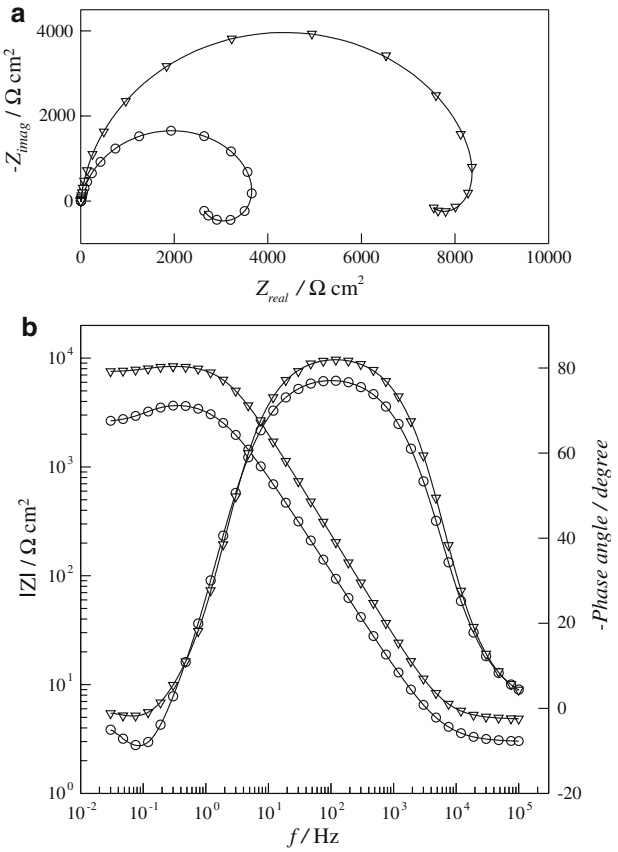

Fig. 6. Nyquist plots (a) and Bode plots (b) of the Al–2.5Mg alloy in a 3% NaCl solution at the E_{OCP} at 20 °C and the flow rate $v = 0.0029$ m s^{-1}, without inhibitor (○) and with the addition of 1×10^{-5} mol dm^{-3} (+)-catechin (▽).

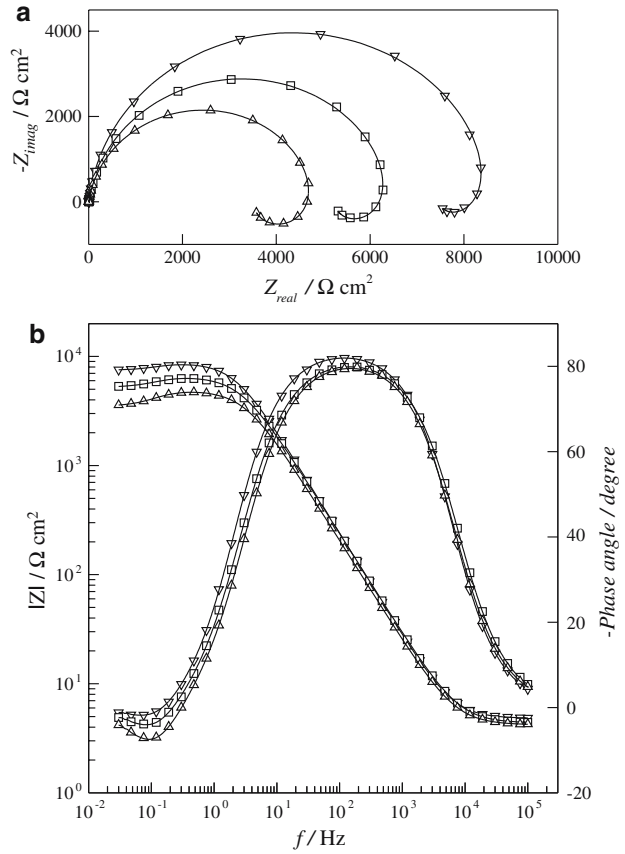

Fig. 7. Nyquist plots (a) and Bode plots (b) of the Al–2.5Mg alloy in a 3% NaCl solution in the presence of 1×10^{-5} mol dm^{-3} (+)-catechin at the E_{OCP} at 20 °C and flow rates $v_1 = 0.0029$ m s^{-1} (∇), $v_2 = 0.0059$ m s^{-1} (□) and $v_3 = 0.0118$ m s^{-1} (Δ).

capacitive semicircle (in the Nyquist plot) and a slight reduction of the absolute impedance value (in the Bode plot). With increase in flow rate the inductive loop becomes more pronounced. In the mathematical analysis of the impedance diagrams, the constant phase element, CPE, was used instead of an "ideal" capacitor to account for the deviations observed as capacitive loops are depressed. The impedance, Z_{CPE}, of CPE is described by the expression [35, 36]

$$Z_{CPE} = Q^{-1}(i\omega)^{-n} \tag{8}$$

with Q and n constants, that can be used in data fitting when interpreting frequency dispersions. The exponent n has values between −1 and 1. The value of −1 is characteristic of an inductance, the value of 1 corresponds to a resistor and the value of 0.5 can be assigned to diffusion phenomena. Figure 8 shows the equivalent circuit used to fit the experimental data. It consists of a CPE in parallel to the series resistors R_1 and R_2 and an inductance L in parallel to R_2. R_{el} corresponds to the electrolyte resistance and was found to be of the order of 4 Ω cm^2.

As a first approximation, R_1 could be used as an evaluation of the corrosion resistance of the system. R_1 corresponds to a low frequency limit of the impedance

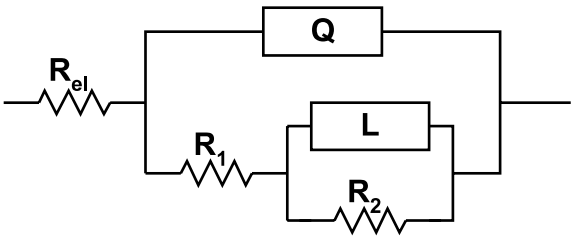

Fig. 8. The equivalent circuit for modelling impedance data of the Al–2.5Mg alloy.

diagrams. In general, this value may be used to obtain the apparent polarization resistance, R_p:

$$R_p = \lim_{\omega \to 0}[Z_{real}] \tag{9}$$

In a simple corrosion system, R_p is determined only by a charge transfer-controlled process. In a more complex system, i.e. in a real three-dimensional nonhomogeneous system [37], (like the present case, where the oxide layer covers the Al alloy), R_p is in general a complicated function determined by the rates of charge transfer, mass transport and chemical reaction [38].

The parameters of the equivalent circuit R_1, Q, R_2, and L were evaluated using the simple least squares fit procedure, and are shown in Table 5. The addition of inhibitor leads to an increase in the value of polarization resistance (R_1) from 2.58 to 7.49 kΩ cm^2. The value of Q decreases from 29.55 to 9.76 × 10^{-6} Ω^{-1} s^n cm^{-2}, while the parameters of the inductive loop R_2 and L decrease slightly. The changes observed are probably due to formation of a thicker and compact protective layer (alloy–oxide–inhibitor) that represents a physical barrier and affects the velocity of local processes at the oxide/electrolyte phase boundary.

With the increased flow velocity of the inhibiting NaCl solution, the value of resistance R_1 significantly decreases from 7.49 to 3.51 kΩ cm^2, while the value of parameter Q increases from 9.76 to 12.95 × 10^{-6} Ω^{-1} s^n cm^{-2}. The parameters of the inductive loop R_2 and L increase slightly with increase in flow rate. These results indicate weaker adsorption of the inhibitor on the electrode surface and lower protective properties of the surface adsorption layer.

Table 5. Impedance parameters for the Al–2.5 Mg alloy in a 3% NaCl solution without and with the presence of inhibitor

c(+)-catechin mol dm^{-3}	v/m s^{-1}	R_{el}/Ω cm^2	Q × 10^6/Ω^{-1} s^n cm^{-2}	n	R_1/kΩ cm^2	L/kH cm^2	R_2/kΩ cm^2
0	0.0029	4	29.55	0.89	2.58	1.56	1.38
1×10^{-5}	0.0029	4	9.76	0.94	7.49	1.51	1.24
1×10^{-5}	0.0059	4	11.16	0.92	5.24	1.60	1.31
1×10^{-5}	0.0118	4	12.95	0.92	3.51	1.64	1.38

4. Conclusions

- A study of the effect of the flow rate and temperature on the corrosion behaviour of the Al–2.5 Mg alloy in a 3% NaCl solution, using the potentiodynamic method and polarization resistance measurements, has shown that increase in flow rate and temperature causes stronger corrosion.
- The addition of (+)-catechin inhibited the corrosion of the Al–2.5Mg alloy in 3% NaCl at all investigated flow rates and temperatures. The inhibiting efficiency decreased with increasing flow rate and temperature.
- Even at the maximum flow rate and the highest temperature (+)-catechin at a concentration of 1×10^{-5} mol dm^{-3} maintains inhibiting properties.

References

1. A.A. Mazhar, W.A. Badawy and M.M. Abou-Romia, *Surf. Coat. Technol.* **29** (1986) 335.
2. W.M. Carroll and C.B. Breslin, *Brit. Corros. J.* **26** (1991) 225.
3. W.A. Badawy, F.M. Al-Kharafi and A.S. El-Azab, *Corros. Sci.* **41** (1999) 709.
4. C. Monticelli, G. Brunoro, A. Frignani and F. Zucchi, *Corros. Sci.* **32** (1991) 693.
5. T.P. Moffat, G.R. Stafford and D.E. Hall, *J. Electrochem. Soc.* **140** (1993) 2779.
6. Y.I. Kuznetsov. *in* J.G.N. Thomas (Ed), Organic Inhibitors of Corrosion of Metals., (Plenum Press, New York, 1996), pp. 107.
7. M. Kliškić, J. Radošević and S. Gudić, *J. Appl. Electrochem.* **27** (1997) 947.
8. W.A. Badawy and F.M. Al-Kharafi, *Corros. Sci.* **39** (1997) 681.
9. M. Bethencourt, F.J. Botana, M.A. Cauqui, M. Marcos, M.A. Rodriguez and J.M. Rodriguez-Izquierdo, *J. Alloys Compounds* **250** (1997) 55.
10. A. Aballe, M. Bethencourt, F.J. Botana and M. Marcos, *J. Alloys Compounds* **323–324** (2001) 855.
11. D. Zhu and W.J. van Ooij, *Corros. Sci.* **45** (2003) 2177.
12. S.S. AbdEl Rehim, H.H. Hassan and M.A. Amin, *Corros. Sci.* **46** (2004) 5.
13. A.A. El-Shafei, M.N.H. Moussa and A.A. El-Far, *J. Appl. Electrochem.* **27** (1997) 1075.
14. G. Bereket and A. Yurt, *Corros. Sci.* **43** (2001) 1179.
15. A.Y. El-Etre, *Corros. Sci.* **43** (2001) 1031.
16. M. Kliškić, J. Radošević, S. Gudić and V. Katalinić, *J. Appl. Electrochem.* **30** (2000) 823.
17. J. Radošević, M. Kliškić and A. Višekruna, *Kem. Ind.* **50** (2001) 537.
18. G.O. Avwiri and F.O. Igho, *Mater. Letts.* **57** (2003) 3705.
19. B. Poulson, *Corros. Sci.* **23** (1983) 391.
20. G. Schmitt, 'Proceedings of the 8th European Symposium of Corrosion Inhibitors, Ferrara', (1995), p. 1075.
21. G. Le Nest, O. Caille, M. Woudstra, S. Roche, B. Burlat, V. Belle, B. Guigliarelli and D. Lexa, *Inorg. Chim. Acta* **357** (2004) 2027.
22. L.F. Wang and H.Y. Zhang, *Bioorg. Chem.* **33** (2005) 108.
23. E. Stupnišek-Lisac, N. Galić and R. Gašparac, *Corrosion* **56** (2000) 1105.
24. C. Monticelli, G. Brunoro and G. Trabanelli, 'Proceedings of the 7th European Symposium on Corrosion Inhibitors, Ferrara', (1990) p. 1125.
25. Z. Grubač, R. Babić and M. Metikoš-Huković, *J. Appl. Electrochem.* **32** (2002) 431.
26. C.M.A. Brett, *J. Appl. Electrochem.* **20** (1990) 1000.
27. C.M.A. Brett, *Corros. Sci.* **33** (1992) 203.
28. J.B. Bessone, D.R. Salinas, C.E. Mayer, M. Ebert and W.J. Lorenz, *Electrochim. Acta* **37** (1992) 2283.
29. J.B. Bessone, C. Mayer, K. Juttner and W.J. Lorenz, *Electrochim. Acta* **28** (1983) 171.
30. S.E. Frers, M.M. Stefanel, C.M. Mayer and T. Chierchie, *J. Appl. Electrochem.* **20** (1990) 996.
31. H.J. de Wit, C. Wijenberg and C. Crevecoeur, *J. Electrochem. Soc.* **126** (1979) 779.
32. G.T. Burstein and R.J. Cinderey, *Corros. Sci.* **32** (1991) 1195.
33. R.J. Cinderey and G.T. Burstein, *Corros. Sci.* **33** (1992) 475.
34. H.J.W. Lenderink, M.V.D. Linden and J.H.W. de Wit, *Electrochim. Acta* **38** (1993) 1989.